Christian Fleßner*

Leonard Thraen

Felix Ziegler

Low-Temperature Correlation of Property Data for Dilute Aqueous Lithium Bromide Solution

A new correlation for some transport properties of aqueous solutions, based on the data published by Sawada et al. [1], is proposed. The main objective of the new fit is to give a smooth transition to the properties of pure water to allow the use of the fit in the region of very dilute solutions. Additionally, the quality of the fit to the experimental data is improved compared to the original correlation. An extrapolation of the new correlation in the other direction, i.e., to higher mass fractions and temperatures, is smooth but does not fully capture the trend described by other experimental datasets. To this end, the correlation has to be refined further.

1 Introduction

The extension of the application range of absorption refrigeration with water as refrigerant to temperatures below 0 °C usually requires an additive in the evaporator to avoid freezing. With lithium bromide (LiBr) already in use as a sorbent, the usage of dilute solutions in the evaporator for this purpose is an evident option. The method has been experimentally proven for refrigeration and heat pump applications (e.g., Kühn et al. [2] and Richter [3]) but is not widely applied yet. To facilitate the design of evaporators with dilute aqueous solutions of LiBr below 0 °C, accurate property correlations for these operating conditions are required.

Sawada et al. [1] have presented measured data and correlations for surface tension σ, dynamic viscosity η, and thermal conductivity λ of aqueous solutions of LiBr and lithium thyocyanate (LiSCN) in the region of interest. The purely empirical correlation has an identical general form for any arbitrary property P_{Sol} of both saline solutions:

$$P_{Sol} = a \, T^b (100 \, \xi)^c \tag{1}$$

with temperature T in K, mass fraction ξ in $kg_{LiBr} kg_{Sol}^{-1}$ and the real coefficients a, b, and c.

The correlation gives implausible results below the lower validity threshold of mass fraction (see Tab. 1). For ξ approaching zero, the correlated values do not meet the data of pure water but they tend to zero or to infinity depending on the sign of the exponent c in Eq. (1).

In order to remove this feature which prohibits the use of the correlation in the region of very dilute solutions, a new correlation based on the experimental data for aqueous lithium

Table 1. Validity ranges of Sawada et al. [1].

	σ	Λ	η
Temperature	255 K $\leq$ T $\leq$ 298 K	268 K $\leq$ T $\leq$ 298 K	263 K $\leq$ T $\leq$ 298 K
Mass fraction	0.05 $\leq$ ξ $\leq$ 0.20	0.10 $\leq$ ξ $\leq$ 0.20	0.05 $\leq$ ξ $\leq$ 0.20

bromide by Sawada et al. [1] is developed. The original form shown in Eq. (1) is extended by normalizing and linking it to the respective property of pure water $P_W(T)$

$$\frac{P_{Sol}}{P_W(T)} = 1 + a\left(\frac{T}{T_C}\right)^b \xi^c \tag{2}$$

with new coefficients fitting the experimental data and meeting per definition the established equations for pure water. Additionally, the temperature is normalized with the critical temperature of water T_C [4] to avoid differences in magnitude between the independent variables temperature and composition.

The data for liquid water extending to subcooled conditions are provided by the IAPWS release R1-76 [5] for surface tension σ and the IAPWS supplementary release SR6-08 [6] respectively Pátek et al. [7] for thermal conductivity λ and dynamic viscosity η. These equations can be reasonably extra-

Christian Fleßner, Leonard Thraen, Prof. Dr. Felix Ziegler
christian.flessner@tu-berlin.de
Technische Universität Berlin, Institut für Energietechnik, Marchstr. 18, 10587 Berlin, Germany.

polated down to 253.15 K. The pressure dependence of liquid aqueous property data at subatmospheric pressure is negligible. Therefore, data recorded at standard atmospheric pressure can be used down to the saturation pressure at the respective temperatures.

2 Method

The original experimental data is manually extracted from the published diagrams of Sawada et al. [1] with WebPlotDigitizer [8]. In the case of thermal conductivity and viscosity, Sawada et al. [1] used data that originate from other sources [9] additionally to their own data for fitting; all these data are employed in this work as well without differentiating between the sources. The data points for pure water ($\xi = 0$) were left out due to the normalization to P_W with the respective sets of equations. Then new coefficients according to Eq. (2) are fitted with the cftool App from MATLAB's curve fitting toolbox [10]. A nonlinear least square method with a trust-region algorithm was applied. No weighting and no outlier detection has been applied. Since varying iteration start values can lead to different solutions, the process was repeated 10 000 times with different random start values. The goodness of fit was determined with the following parameters provided by MATLAB (Field [11], nomenclature adapted to MATLAB):

DFE: The degree of freedom for residuals respectively errors (DFE) is the difference between the number of measured values. The correlation is based on n and the number of estimated coefficients, m (Eq. (3)). This parameter is reported in Tab. 3 to facilitate the assessment of the other parameters.

$$DFE = n - m \qquad (3)$$

SSE/RMSE: The residual sum of squares or sum of squares estimate of errors (SSE) is the sum of squares of the difference between the observed data y_i and the value predicted by the model $\hat{y}_i$ (Eq. (4)). The root-mean-square deviation or error (RMSE) relates the root of this difference to the degree of freedom for residuals (see Eqs. (3) and (5)). These parameters have to be minimal. Since both are closely related, only RMSE is reported in Tab. 3.

$$SSE = \sum_{i=1}^{n} \left(y_i - \hat{y}_i \right)^2 \qquad (4)$$

$$RMSE = \sqrt{\frac{\sum_{i=1}^{n} \left(y_i - \hat{y}_i \right)^2}{DFE}} \qquad (5)$$

$R^2/R_{adj.}^2$: The coefficient of determination R^2 describes the proportion of the variance in the dependent variable that is predictable from the independent variables (Eq. (6)). The adjusted coefficient of determination $R_{adj.}^2$ accounts for the relation of the number of data points to the number of parameters (Eq. (7)). Since the degree of freedom for residuals is close to the number of data points for all investigated properties, this parameter deviates only slightly from the coefficient of determination. Therefore, only this value is reported in Tab. 3. These parameters are optimal for a value of 1.

$$R^2 = 1 - \frac{\sum_{i=1}^{n} \left(y_i - \hat{y}_i \right)^2}{\sum_{i=1}^{n} \left(y_i - \bar{y} \right)^2} \qquad (6)$$

$$R_{adj.}^2 = 1 - \frac{(n-1)}{DFE} \frac{\sum_{i=1}^{n} \left(y_i - \hat{y}_i \right)^2}{\sum_{i=1}^{n} \left(y_i - \bar{y} \right)^2} \qquad (7)$$

Afterwards the best fit was selected by a minimum/maximum search within the stored goodness of fit parameters. In all cases the selected fit was optimal in all four evaluated parameters.

Finally, diagrams are plotted for all three properties over temperature and mass fraction. Isosteric and isothermal lines are shown which have been computed with both the original correlations and the newly fitted correlations. The experimental values of Sawada et al. [1] and selected other experimental values are added to the diagrams. In order to compare the correlation to measured data deviating slightly from defined isothermal and isosteric lines, the data points for plotting are selected with a tolerance of $\Delta\xi = \pm 0.005$ along the isosteric lines and a tolerance of $\Delta T = \pm 1\,K$ along the isothermal lines. Consequently, the diagrams with temperature as abscissa always show all measured data from Sawada et al. [1], whereas the diagrams with mass fraction as abscissa leave out some data points deviating from the chosen isothermal lines since the temperature interval of Sawada et al. [1] is smaller than the chosen interval for isothermal lines. Where deviating concentrations within the tolerance are reported, this is shown in the figure's legend. The crystallization line was plotted using the mass fraction and temperature of crystallization calculated with the correlation by Patek and Klomfar [12] inserted into the new correlation.

3 Results

Tab. 2 shows the fitted parameters of Eq. (2) for all properties rounded to four valid digits. Using more digits has not led to a significant improvement of the correlation. All diagrams have been plotted with this set of parameters.

Table 2. Coefficients of best fits.

	σ	λ	η
a	0.02386	−1.251	301.7
b	−2.951	0.5827	5.738
c	0.8455	1.209	1.389

Tab. 3 presents the results for goodness of fit for the new correlation as well as for the original correlation. The goodness of fit is calculated for $y = P_{Sol}/P_W$ for both correlations. The fit for surface tension σ is excellent for both correlations. The new correlation fits better than the original correlation. The experimental scatter is low and the approach is well suited to reproduce the evolution with temperature as well as with mass fraction. The fit for thermal conductivity λ has a root-mean-square

Table 3. Goodness-of-fit parameters.

	σ		λ		η	
	New correlation	Original correlation	New correlation	Original correlation	New correlation	Original correlation
DFE	32	32	34	34	71	71
RMSE	0.001839	0.006025	0.01078	0.01193	0.04843	0.2324
$R_{adj.}^2$	0.9928	0.9227	0.9561	0.8239	0.8021	−3.558

deviation that is nearly a magnitude higher. The adjusted coefficient of determination is also worse than for surface tension.

The new correlation's goodness of fit for thermal conductivity is slightly better than that of the original correlation. The goodness of fit for dynamic viscosity η is worse yet. This can be attributed to a higher experimental uncertainty resulting in more scatter. The root mean square deviation for the original correlation is nearly a magnitude higher than for the new correlation. The original correlation's adjusted coefficient of determination is negative, therefore indicating that the average value provides a better fit than the correlation. Overall, the new correlation's goodness-of-fit parameters for all properties are in a range that indicates the suitability of the equation's form to capture the dependence of all properties on temperature and composition within the selected range.
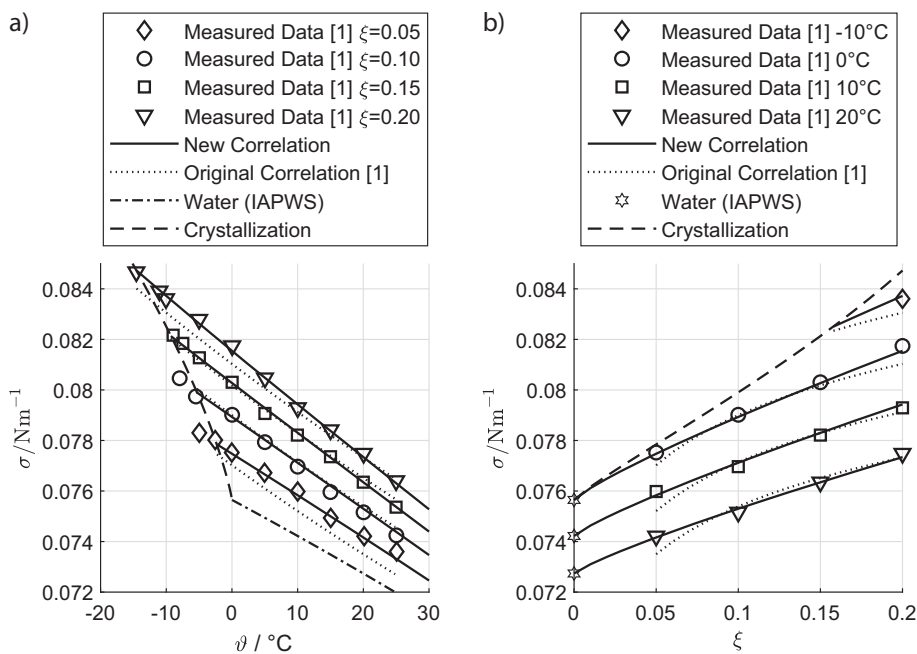
3.1 Surface Tension

The plot of surface tension over temperature in Fig. 1a shows a good agreement of measured and experimental values espe-

cially for the new correlation. The experimental data shows only little scatter. However, a significant deviation of the original correlation to the experimental values is visible at the lower boundary of its validity ($\xi = 0.05$). Finally, it is observed that some data points lie in the area beyond the crystallization limit. It is not sure whether these data points can be attributed to subcooled conditions or experimental uncertainty. Nevertheless, they have not been excluded from the data set for fitting.

The same data plotted over mass fraction in Fig. 1b gives a good impression of the increasing deviation of the original correlation towards its limits of validity whereas the new correlation gives a smooth transition to the surface tension of pure water (marked with a star).

The deviation between measured and calculated surface tension is illustrated in Fig. 2. The original correlation predicts measured data with a maximum deviation from −1.5 % to +0.5 %. The new correlation gives even better results with a maximum deviation of ± 0.5 %.

3.2 Thermal Conductivity

The plot of thermal conductivity over temperature in Fig. 3a shows a significant scatter of the experimental data. Regarding temperature dependence, both correlations show similar agreement to the data.

Fig. 3b indicates thermal conductivity against composition. Within the validity range of the original correlation the experimental data is reproduced adequately by both correlations. However, the extrapolated original correlation tends to infinity for $\xi \to 0$ whereas the new correlation has a smooth transition to the properties of pure water for the respective temperature marked with a star.

The relative deviation of experimental and calculated data for thermal conductivity is similar for both correlations as demonstrated in Fig. 4. Despite the higher scatter in experimental data resulting in mediocre goodness-of-fit parame-
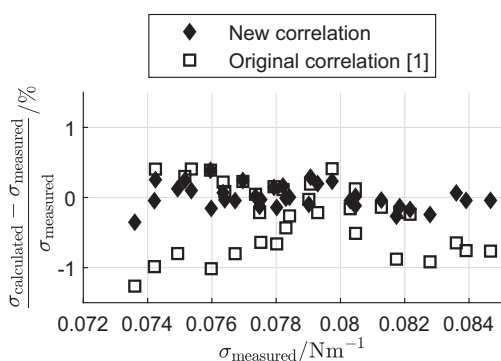

Figure 1. Surface tension plotted against temperature (a) and mass fraction (b). Measured values from Sawada et al. [1]. Isosteric lines for both correlations in (a) 0.05, 0.10, 0.15, and 0.20 increasing from bottom to top. Isothermal lines for both correlations in (b) −10 °C, 0 °C, 10 °C, and 20 °C increasing from top to bottom.
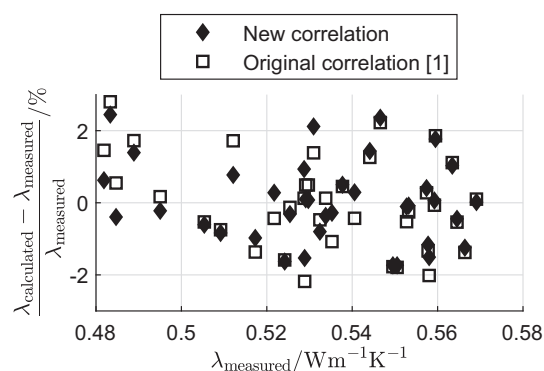
Figure 2. Deviation from measured data of surface tension calculated with the original correlation [1] and the new correlation.

ters seen in Tab. 3, the maximum deviation of both correlations is in the range from −2.5 % to +3 %.

3.3 Dynamic Viscosity

Fig. 5a displays the experimental data reported by Sawada et al. [1] and the original as well as the new correlation for viscosity over temperature for different mass fractions. The experimental data exhibits a larger relative scatter compared to the other properties. Both correlations reproduce the basic trend of the temperature dependence of viscosity. The isosteric lines of the original correlation, however, do not capture the absolute values of the data, whereas the new correlation follows the experimental data more closely. Some experimental values between
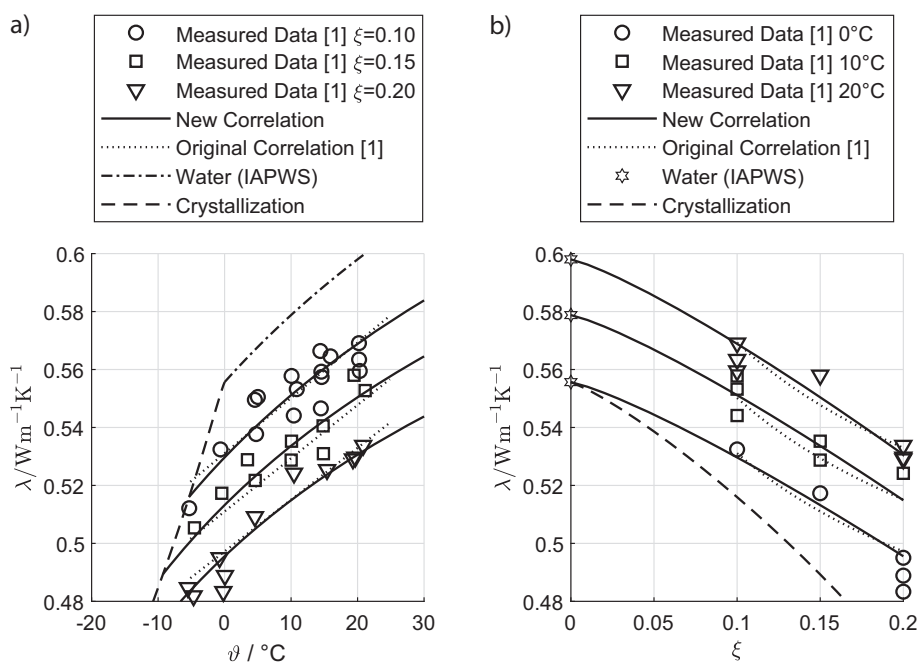

Figure 3. Thermal conductivity plotted against temperature (a) and mass fraction (b). Measured values from Sawada et al. [1]. Isosteric lines for both correlations in (a) 0.10, 0.15, and 0.20 increasing from top to bottom. Isothermal lines for both correlations in (b) 0 °C, 10 °C, and 20 °C increasing from bottom to top.

Figure 4. Deviation from measured data of thermal conductivity calculated with the original correlation [1] and the new correlation.

0 °C and 10 °C for $\xi = 0.05$ indicate a lower viscosity than for pure water at the same temperature. Since this is not supported by other data available in this temperature and concentration range [13, 14], measurement error is a more plausible explanation than an actual physical effect.

In the mass fraction and temperature range considered for this correlation, the influence of mass fraction on viscosity is low compared to the influence of temperature. This is visible in the close stacking of isosteric lines in Fig. 5a as well as in the rather flat slope of isothermal lines in Fig. 5b.

The plot of this data set over mass fraction in Fig. 5b gives more insight where the original correlation fails to predict viscosity. The curvature of the fitting correlation is reversed compared to the experimental data except for 0 °C and a significant offset is visible compared with experimental data. The new correlation follows the experimental data more closely but still does not reproduce all data points. Since no uncertainty of experimental values is reported in the original publication [1], it is not possible to assess this deviation properly, but it seems that the outlying data point at 0 °C and $\xi = 0.05$ is not reliable. For future investigations, more data covering this range should be included into the correlation. Using an outlier detection to exclude such data points from the correlation might also be an option.

Due to the more pronounced scatter of experimental data for viscosity, the goodness of fit represented by the parameters in Tab. 3 is the worst of all properties investigated in this article. The deviation of the original correlation from experimental data shown in Fig. 6 is rather pronounced. It ranges

a)

b)
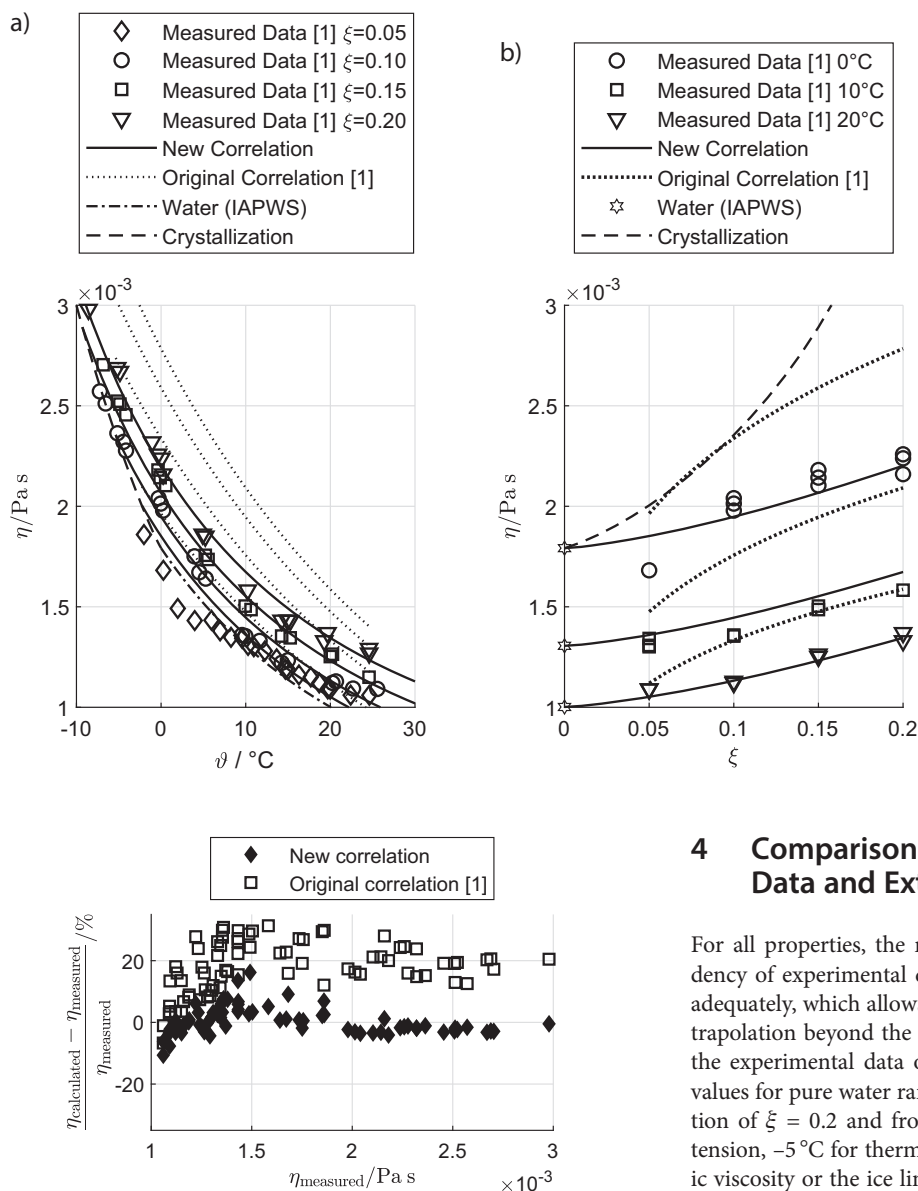
Figure 5. Dynamic viscosity plotted against temperature (a) and mass fraction (b). Measured values from Sawada et al. [1]. Isosteric lines for both correlations in (a) 0.05, 0.10, 0.15, and 0.20 increasing from bottom to top. Isothermal lines for both correlations in (b) 0 °C, 10 °C, and 20 °C increasing from top to bottom.

Figure 6. Deviation from measured data of dynamic viscosity calculated with the original correlation [1] and the new correlation.

from –7 % to +32 % with a systematic tendency to overpredict viscosity. However, since an accuracy of ± 10 % is claimed for the original correlation together with the negative adjusted coefficient of determination (see Tab. 3), a typographic error in the original publication seems plausible. The new correlation results in deviations from –11 % to +17 % with no systematic bias. This is a significant improvement as compared to the original correlation in addition to the feature of capturing the data of pure water.

4 Comparison to other Experimental Data and Extrapolation

For all properties, the new correlation reproduces the dependency of experimental data on temperature and mass fraction adequately, which allows to check the possibility of a decent extrapolation beyond the range of validity. The validity based on the experimental data of Sawada et al. [1] and the calculated values for pure water ranges from pure water up to a mass fraction of $\xi = 0.2$ and from a temperature of –15 °C for surface tension, –5 °C for thermal conductivity, and –10 °C for dynamic viscosity or the ice line, up to 25 °C. For a qualitative assessment of a possible extrapolation, the new correlation is compared with other experimental data. A range of 0 °C to 40 °C and $\xi = 0$ to $\xi = 0.4$ is chosen for the comparison of the extrapolated new correlation.

4.1 Surface Tension

Surface tension without additives close to the validity range of Sawada et al. [1] is available from Yao et al. [15]. The compilation of data by Uemura [16] is an additional source of data over a wide range overlapping with the region of interest. The surface tension data of Löwer [13] was not used for the comparison since these are not primarily experimental but an extrapolation from measured surface tension data of pure water using measured viscosity data of aqueous lithium bromide solution (see Shishkin [17]).

Fig. 7a illustrates that a moderate extrapolation of the new correlation to higher temperatures is reasonable when compared to the experimental data of Yao et al. [15] and Uemura [16]. All experimental data sets agree mostly well in the overlapping range, though the data of Yao et al. [15] show some visible deviation from both other sets at $\xi = 0.1$. The comparison of the isosteric lines for $\xi = 0.3$ and $\xi = 0.4$ with the data of Yao et al. reveals that the potential of extrapolation to higher mass fractions of lithium bromide is rather limited. In this range, the deviation is quickly increasing.

The limits of extrapolation to higher mass fractions are emphasized by plotting against mass fraction (Fig. 7b). The increase in surface tension with salt content given by the correlation is much smaller than the trend of the measured data from Yao et al. [15] and Uemura [16].

4.2 Thermal Conductivity

For the comparison of thermal conductivity with literature several sources are available. Löwer [13] measured a range of properties for aqueous lithium bromide solution including thermal conductivity and viscosity. Zaytsev and Aseyev [14] give a compilation of averaged measured and calculated values for a wide range of salts from several mostly Russian sources. These data sets have a broad overlap with the data of Sawada et al. [1]. Bleazard et al. [18], DiGuilio et al. [19], and DiGuilio and Teja [20] provide data only for a small part of the desired low temperature and mass fraction range. Kawamata et al. [21] provide primarily data for higher temperature and mass fraction ranges and focus on the investigation of pressure dependence. Riedel [22] investigated the concentration dependence

of thermal conductivity at a temperature of 20 °C. The data of Valyashko [23] are not considered since they are completely outside of the considered range. The two more comprehensive experimental datasets [13, 14] agree well with each other and with the data of Sawada et al. [1]. The additional data [18–22] is also qualitatively consistent with the other data sets. Up to a mass fraction of $\xi = 0.2$ the new correlation fits well with the experimental data even when extrapolated to 40 °C (see Fig. 8a). For higher mass fractions (isosteric lines for $\xi = 0.3$ and $\xi = 0.4$) the deviation increases with rising temperature and mass fraction.

The increasing deviation of the new correlation from experimental data with rising mass fraction is also visible in Fig. 8b. The isothermal data of Riedel [22] are almost indiscernible from Löwer's respective data at 20 °C. Since all experimental data sets considered here are qualitatively consistent to each other, it is promising to improve the fit further and use them for an extended fit across the full range of experimental data. This, however, is beyond the scope of the paper at hand.

4.3 Dynamic Viscosity

For the comparison of dynamic viscosity, the situation is similar to thermal conductivity. The measured data of Löwer [13] and the compilation of Zaytsev and Aseyev [14] cover a wide range of relevant data. The often cited data of Lee et al. [24] considers a minimal mass fraction of $\xi_{min} = 0.45$ and is therefore outside the scope of this comparison. The data sets of Rohman et al. [25], Lo Surdo and Wirth [26], and Wimby and Berntsson [27] provide data for a limited section of the desired range, which is included in Fig. 9.
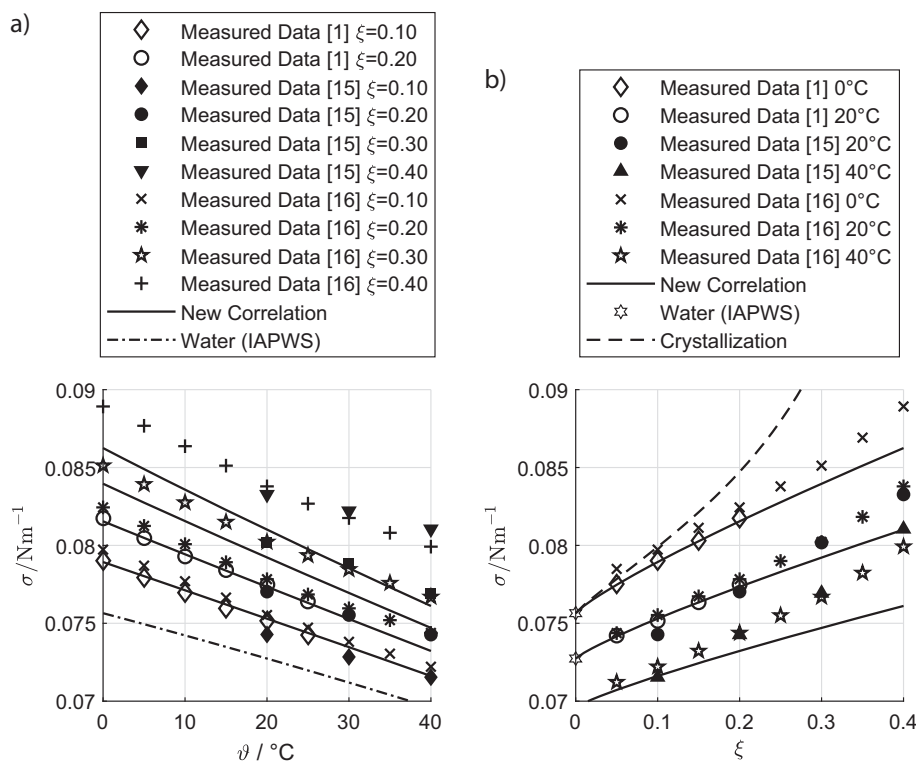
Figure 7. Surface tension plotted against temperature (a) and mass fraction (b) with experimental data from Sawada et al. [1], Yao et al. [15], and Uemura [16] for different mass fractions with extrapolated new correlation. Isosteric lines in (a) 0.1, 0.2, 0.3, and 0.4 increasing from bottom to top. Isothermal lines in (b) 0 °C, 20 °C, and 40 °C increasing from top to bottom.
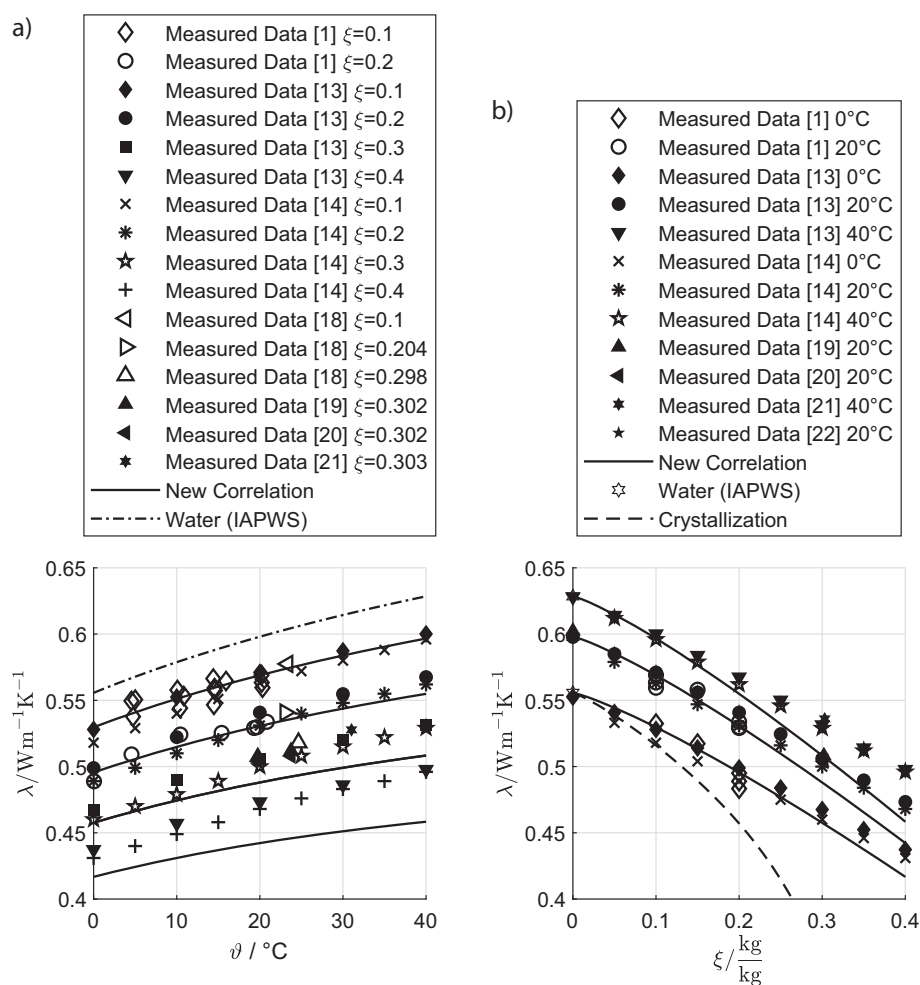
Figure 8. Thermal conductivity plotted against temperature (a) and mass fraction (b) with experimental data from Sawada et al. [1], Löwer [13], Zaytsev and Aseyev [14], Bleazard [18], Di Guilio et al. [19], Di Guilio and Teja [20], Kawamata et al. [21], and Riedel [22] for different mass fractions with extrapolated new correlation. Isosteric lines in (a) 0.1, 0.2, 0.3, and 0.4 increasing from top to bottom. Isothermal lines in (b) 0 °C, 20 °C, and 40 °C increasing from bottom to top.

For lower temperatures the data of Zaytsev and Aseyev [14] diverge from Löwer's [13] data in the intermediate mass fraction range (isosteric lines for $\xi = 0.2$ and $\xi = 0.3$) while showing the same trend as seen in Fig. 9a. Otherwise, all data sets show qualitatively good agreement in Fig. 9a. The temperature dependence of the experimental data sets is well captured by the new correlation within its validity range concerning mass fraction. Extrapolation up to 40 °C thus seems reasonable. For $\xi = 0.3$ and $\xi = 0.4$ an increasing deviation is visible especially in the low temperature range.

The dependence of viscosity on mass fraction of LiBr in comparison to experimental data sets is demonstrated in Fig. 9b. For the 30 °C and 40 °C isothermal lines, the new correlation can be reasonably extrapolated to a mass fraction up to $\xi = 0.4$. For lower temperatures the deviation increases, showing the limits of the new correlation's extrapolation above $\xi = 0.3$. The deviation of Zaytsev's and Aseyev's [14] data to Löwer's [13] data in the intermediate mass fraction range is clearly visible for 0 °C. The measured viscosity of Rohman et al. is systematically lower than all other data, with lower measured viscosity than for pure water for solutions below $\xi = 0.1$. A further critical evaluation of viscosity measurements is sensible but beyond the scope of the present study.

5　Conclusion

The goal of the new correlation was reached, i.e., the correlation interpolates smoothly in the region between pure water and experimental data of aqueous solutions. At the same time, the quality of the fit is not jeopardized. On the contrary, the new correlation agrees equally well or better with the experimental data by Sawada et al. [1] than the original correlation. The new correlation compares well to other experimental data sets within its validity range and can be extrapolated up to temperatures of 40 °C. The extrapolation of the new correlation to higher mass fractions is not recommendable. Above $\xi = 0.2$ the deviation increases significantly. Consequently, the dependency on composition should be investigated further, when the correlation is to be used for a salt mass fraction larger than $\xi = 0.2$. This, however, is not the area of interest here.

The experimental data by Sawada et al. [1] for viscosity have a large scatter. This makes the evaluation of the new correlation's accuracy somewhat difficult. New more accurate data within the required temperature range is desirable, since no published data in this range is available.

a)

b)
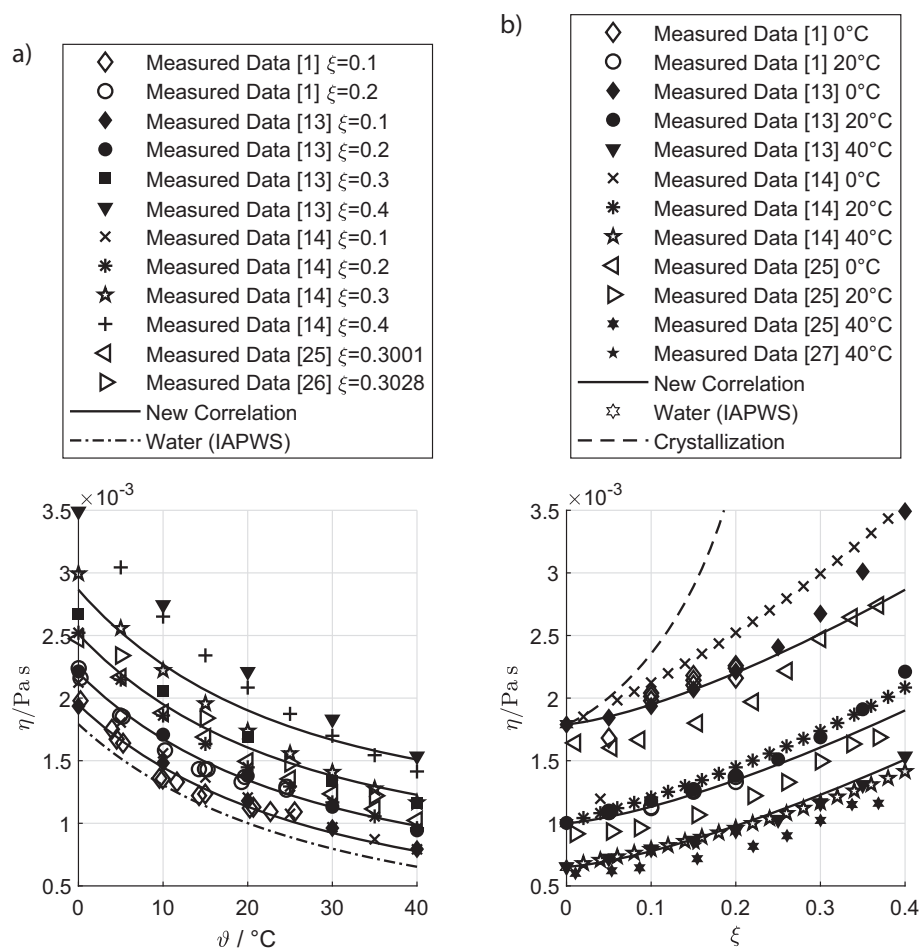
Figure 9. Dynamic viscosity plotted against temperature (a) and mass fraction (b) with experimental data from Sawada et al. [1], Löwer [13], Zaytsev and Aseyev [14], Rohman et al. [25], Lo Surdo and Wirth [26], and Wimby and Berntsson [27] for different mass fractions with extrapolated new correlation. Isosteric lines in (a) 0.1, 0.2, 0.3, and 0.4 increasing from bottom to top. Isothermal lines in (b) 0 °C, 20 °C, and 40 °C increasing from top to bottom.

Since the different experimental data sets considered for this article agree generally well, an extension of the basic formulation with additional input for the data fit is promising.

Data Availability Statement

The data that support the findings of this study are available from the corresponding author upon reasonable request.

Acknowledgment

The authors have declared no conflict of interest.

Symbols used

a, b, c	[–]	fitting coefficients in Eqs. (1) and (2)
i	[–]	index
m	[–]	number of estimated coefficients
n	[–]	number of measured values
P	[–]	arbitrary property
R^2	[–]	coefficient of determination
T	[K]	temperature
y_i	[–]	observed response to independent variables
$\hat{y}_i$	[–]	predicted response from independent variables
$\bar{y}$	[–]	average value of observed response to independent variables

Greek letters

η	[Pa s]	surface tension
λ	[W m^{-1}K^{-1}]	thermal conductivity
ϑ	[°C]	temperature
ξ	[kg$_{LiBr}$kg$_{Sol}^{-1}$]	mass fraction of lithium bromide
σ	[N m^{-1}]	surface tension

Sub- and superscripts

adj.	adjusted
calculated	value predicted with a correlation
LiBr	lithium bromide
measured	measured value
min	minimal
Sol	solution
W	water

Abbreviations

DFE	degree of freedom for residuals
RMSE	root-mean-square deviation
SSE	residual sum of squares

References

[1] I. Sawada, M. Yamada, S. Fukusako, T. Kawanami, *Int. J. Thermophys.* **1998**, *19 (3)*, 749–759. DOI: https://doi.org/10.1023/A:1022626503214

[2] A. Kühn, T. Meyer, F. Ziegler, *9th Int. IEA Heat Pump Conf.*, Zürich **2008**, 5.41.

[3] L. Richter, *KI Kälte Luft Klimatechnik* **2008**, *3*, 26–29.

[4] W. Wagner, A. Pruss, *J. Phys. Chem. Ref. Data* **1993**, *22 (3)*, 783–787. DOI: https://doi.org/10.1063/1.555926

[5] R1-76, *Revised Release on Surface Tension of Ordinary Water Substance*, IAPWS, **2014**.

[6] SR6-08, *Revised Supplementary Release on Properties of Liquid Water at 0.1 MPa*, IAPWS, **2011**.

[7] J. Pátek, J. Hrubý, J. Klomfar, M. Soucková, A. H. Harvey, *J. Phys. Chem. Ref. Data* **2009**, *38 (1)*, 21–29. DOI: https://doi.org/10.1063/1.3043575

[8] A. Rohatgi, *Webplotdigitizer: Version 4.3*, https://automeris.io/WebPlotDigitizer, **2020**.

[9] *Thermophysical Properties Handbook*, Japan Society of Thermophysical Properties, Yokendo, Tokyo **1992**.

[10] The MathWorks Inc., MATLAB R2019b Curve Fitting Toolbox, **2019**.

[11] A. Field, *Discovering Statistics Using IBM SPSS Statistics*, Sage Publications, London **2018**.

[12] J. Pátek, J. Klomfar, *Fluid Phase Equilib.* **2006**, *250, 1–2*, 138–149. DOI: https://doi.org/10.1016/j.fluid.2006.09.005

[13] H. Löwer, Thermodynamische und physikalische Eigenschaften der wässrigen Lithiumbromidlösung, *Ph.D. Thesis*, Technische Hochschule Karlsruhe **1960**.

[14] *Properties of Aqueous Solutions of Electrolytes* (Eds: I. D. Zaytsev, G. G. Aseyev), CRC Press, Boca Raton, FL **1992**.

[15] W. Yao, H. Bjurstroem, F. Setterwall, *J. Chem. Eng. Data* **1991**, *36 (1)*, 96–98. DOI: https://doi.org/10.1021/je00001a029

[16] M. Uemura, *Refrigeration (Japan)*, **1977**, *52*, 600.

[17] A. Shishkin, *9th Russian-Korean Int. Symp. on Science and Technology*, Novosibirsk **2005**, 280–283. DOI: https://doi.org/10.1109/KORUS.2005.1507708

[18] J. G. Bleazard, R. M. DiGuilio, A. S. Teja, in *Thermophysical Properties for Industrial Process Design* (Eds: T. B. Selover, C. C. Chen), AIChE Symposium Series 298, American Institute of Chemical Engineers, New York **1994**, 23–28.

[19] R. M. DiGuilio, R. J. Lee, S. M. Jeter, A. S. Teja, *ASHRAE Trans.* **1990**, *96*, 702–708.

[20] R. M. DiGuilio, A. S. Teja, *Ind. Eng. Chem. Res.* **1992**, *31 (4)*, 1081–1085. DOI: https://doi.org/10.1021/ie00004a016

[21] K. Kawamata, Y. Nagasaka, A. Nagashima, *Int. J. Thermophys.* **1992**, *9 (3)*, 317–329. DOI: https://doi.org/10.1007/BF00513074

[22] L. Riedel, *Chem. Ing. Tech.* **1951**, *23 (3)*, 59–64. DOI: https://doi.org/10.1002/cite.330230303

[23] V. M. Valyashko, *Hydrothermal Properties of Materials*, John Wiley & Sons, Chichester, UK **2008**.

[24] R. J. Lee, R. M. DiGuilio, S. M. Jeter, A. S. Teja, *ASHRAE Trans.* **1990**, *96*, 709–714. DOI: https://doi.org/10.1016/S0167-7322(02)00047-8

[25] N. Rohman, N. N. Dass, S. Mahiuddin, *J. Mol. Liq.* **2002**, *100*, 265–290.

[26] A. Lo Surdo, H. E. Wirth, *J. Phys. Chem.* **1979**, *83 (7)*, 879, 888. DOI: https://doi.org/10.1021/j100470a024

[27] J. M. Wimby, T. S. Berntsson, *J. Chem. Eng. Data* **1994**, *39 (1)*, 68–72. DOI: https://doi.org/10.1021/je00013a019